JOURNAL OF APPLIED ELECTROCHEMISTRY 17 (1987) 156–164

Electroplating of antimony and antimony–tin alloys

S. S. ABD EL REHIM

Department of Chemistry, Faculty of Science, Ain Shams University, Abbasia, Cairo, Egypt

A. AWAD, A. EL SAYED

Department of Chemistry, Faculty of Science, Assiut University, Assiut, Egypt

Received 23 December 1985; revised 24 February 1986

The electroplating of antimony from $KSb(OH)_6$ and antimony–tin alloys from mixtures of $KSb(OH)_6$ and $Na_2Sn(OH)_6$ onto steel substrates has been investigated under variable plating conditions. The influence of added tartaric acid, current density and temperature on cathodic potentials, cathodic current efficiencies, appearance of the deposits and chemical composition of the alloys has been studied. X-ray diffraction analysis has showed that amorphous or hexagonal antimony deposits are produced from solutions free from or containing tartaric acid. The alloy deposit (56% antimony) was produced in rhombohedral crystal structure. Fine-grained, highly adherent and dark-greyish deposits of antimony and antimony–tin alloys were plated in most cases.

1. Introduction

The high corrosion resistance, high metallic lustre and wide range of applications [1] of antimony and its alloys make their electrodeposition of practical importance. Concentrated acids do not dissolve the metal but rather oxidize it to insoluble trioxide or pentoxide [2]. Alkalis have no significant effect on the metal [3].

Antimony can be electrodeposited from a wide variety of plating baths including citrate [3–5], tartrate [6, 7], fluoride [8], chloride [9, 10] and fluoborate [11]. The protective value of the deposits is comparable to that of nickel deposits [3, 8]. Frequently the deposits are cracked, especially the bright deposits. However, Fedot'ev and co-workers [3] claimed that crack-free deposits can be deposited in the presence of some organic additions.

Several baths have been proposed for the electrodeposition of antimony–tin alloys. Cuthbertson and Parkinson [12] deposited the alloy from fluoride. The alloys were bright and white and the brightness increased with temperature. Kudryavtsev and co-workers [13, 14] electrodeposited the alloy onto a steel substrate from acid electrolyte containing NH_4F, and fine crystal-structure deposits were obtained, Kushnir *et al.* [15] also obtained crystal blocks of the alloy from aqueous solution containing $SbCl_3$, $SnCl_2$ and NH_4F. However, Izbekova *et al.* [16] produced high quality deposits from a bath containing sodium pyrophosphate, $SbCl_3$ and $SnCl_2$ in the presence of some organic additions at pH 5.5. Monk and Ellingham [17] deposited the alloy from alkali stannate–thioantimonate solutions at 15–70° C. The deposits contained sulphur and were brittle.

Continuing our work on the electroplating of some metals and alloys [18–22], the present study was undertaken to investigate the electrodeposition of antimony from $KSb(OH)_6$ and antimony–tin alloy from $KSb(OH)_6$–stannate baths under different conditions.

2. Experimental details

For antimony deposition, the plating baths were prepared from $KSb(OH)_6$ free from or containing tartaric acid ($H_2C_4H_4O_6$). For the alloy deposition, the solutions were prepared from $KSb(OH)_6$, $Na_2Sn(OH)_6$ and $H_2C_4H_4O_6$; the pH of each alloy bath was measured using an Orion Research digital ionalyser (Model 501) and adjusted to 7.4 by means of KOH solution.

0021–891X/87 $03.00 + .12

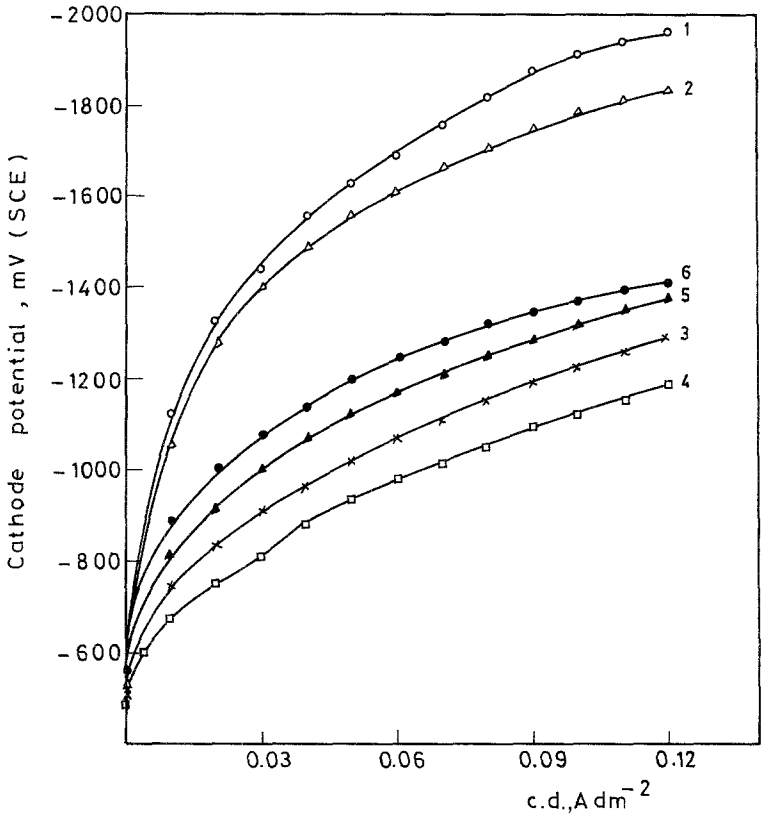

Fig. 1. Cathodic polarization curves for antimony. Curve 1, 20 g l^{-1} $KSb(OH)_6$, pH 11.2, 30° C; curve 2, 20 g l^{-1} $KSb(OH)_6$, pH 11.2, 50° C; curve 3, 20 g l^{-1} $KSb(OH)_6$ + 40 g l^{-1} $H_2C_4H_4O_6$, pH 2.1, 30° C; curve 4, 20 g l^{-1} $KSb(OH)_6$ + 40 g l^{-1} $H_2C_4H_4O_6$, pH 2.1, 50° C; curve 5, 20 g l^{-1} $KSb(OH)_6$ + 40 g l^{-1} $H_2C_4H_4O_6$, pH 7.4, 50° C; curve 6, 20 g l^{-1} $KSb(OH)_6$ + 40 g l^{-1} $H_2C_4H_4O_6$, pH 7.4, 30° C.

All the solutions were prepared from Analar chemicals using distilled water.

A double-wall cylindrical (Pyrex) container of capacity 500 ml, fitted with a lid, was used as the plating cell. The lid had three openings for the insertion of a platinum anode, a low carbon steel cathode and a salt bridge. The area of each electrode was 2.5 × 3 cm^2. Fresh electrodes and solution were used for each run. All experiments were conducted at a constant temperature of ± 0.5° C. The potentials were measured using a saturated calomel electrode (SCE) as a reference and an Einstel Widerstande Ruhstrate K.G. (Model 3401) potentiometer.

The quantity of electricity was determined coulometrically. Each cathode was washed thoroughly after each deposition with distilled water, then dried and weighed. The cathode efficiency of the alloys was determined by a recommended method [23]. Dissolution of the alloy deposit from the cathode was carried out by 1 : 1 HCl and a few drops of H_2O_2. The tin content of the deposit was determined by atomic absorption spectrophotometric analysis (Perkin Elmer 4000) at wave length 286.3 Å, making use of EDL absorbance. The antimony content was determined by weight difference.

The morphology of the as-plated deposits was examined with a scanning electron microscope (JEOL Model 50 A). X-ray diffraction analysis of the deposits was performed using a Philips diffractometer (30 kV, 20 mA) with an iron filter and cobalt radiation. The microhardness of the coated specimen was measured by means of a Leitz–Wetzlar type microhardness tester with a Vickers diamond indenter. In all tests a load of 50 g was employed and the hardness was expressed as a Vickers hardness number (VHN).

3. Results and discussion

The cathodic potential–current density curves for antimony deposition from $KSb(OH)_6$ (20 g l^{-1}) devoid of or containing 40 g l^{-1} $H_2C_4H_4O_6$ onto steel substrates at different pH values and temperatures are given in Fig. 1.

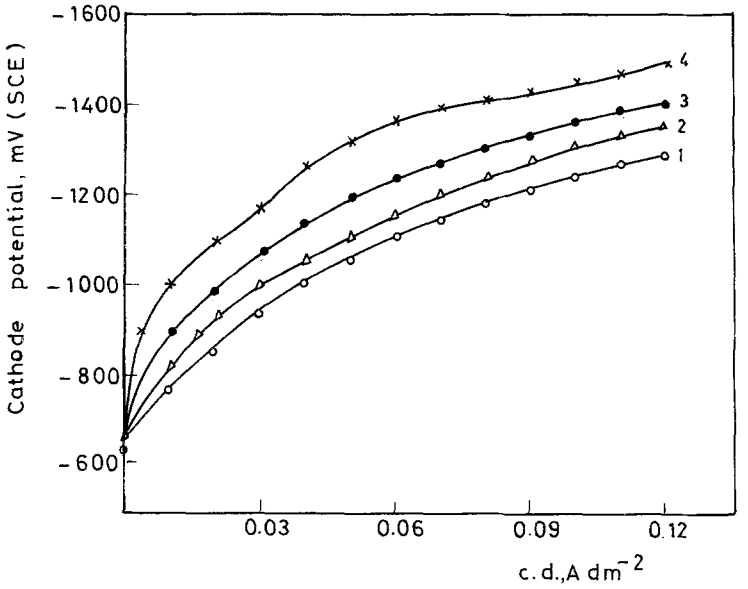

Fig. 2. Cathodic polarization curves of antimony at 30° C from solution containing 40 g l^{-1} $H_2C_4H_4O_6$ at pH 7.4. Concentrations of $KSb(OH)_6$: curve 1, 5 g l^{-1}; curve 2 10 g l^{-1}; curve 3, 20 g l^{-1}; curve 4, 25 g l^{-1}.

The curves show that antimony was deposited with significant cathodic polarization or metal deposition overvoltage. Simultaneous discharge of hydrogen ions was observed during the deposition of the metal. Inspection of the data obtained reveals that the cathodic polarization increases with increasing current density and decreases with temperature. Addition of the acid and lowering the pH of the bath also decreases the cathodic polarization.

Fig. 2 illustrates the influence of $KSb(OH)_6$ concentration on the cathodic polarization of antimony. Under a given condition of acid concentration (40 g l^{-1}), pH (7.4) and temperature (30° C), the cathodic polarization increases with increasing the antimony content of the bath.

The cathodic current efficiency of antimony deposition from these solutions was determined and the results are presented in Figs 3 and 4. The cathode efficiency is generally low indicating preferential discharge of hydrogen ions. This efficiency increases with increasing current density but decreases with increasing bath

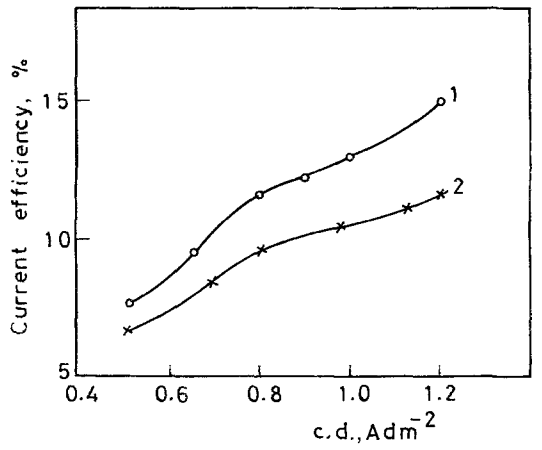

Fig. 3. Cathodic efficiency of antimony from solution containing 20 g l^{-1} $KSb(OH)_6$ and 40 g l^{-1} $H_2C_4H_4O_6$ at pH 7.4 and plating time 30 min. Curve 1, 30° C; curve 2, 50° C.

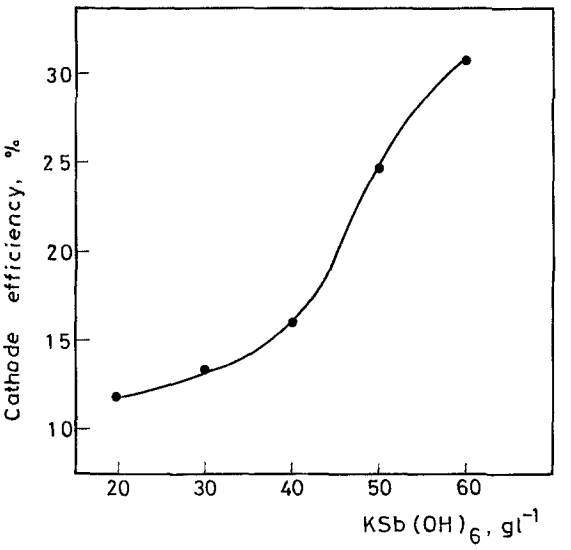

Fig. 4. Cathodic efficiency of antimony deposited from solution containing 40 g l^{-1} $H_2C_4H_4O_6$ at pH 7.4, 30° C, 0.8 A dm^{-2} and varying concentration of $KSb(OH)_6$.

Table 1. X-ray diffraction patterns of Sb and Sb–Sn alloy deposited at 0.8 A dm^{-2} and 30° C for 60 min on steel cathodes

Solution	*Conc.* ($g l^{-1}$)	*Deposit*	*d-spacing* (Å)	*Relative intensity* I/I_0	*hkl*	*Lattice parameters* (Å)		*System*
						a	*c*	
$KSb(OH)_6$	20	Sb						amorphous
$KSb(OH)_6$	20	Sb	2.86	35.8	010	3.31	5.3	hexagonal
			2.65	29.5	002			
$+H_2C_4H_4O_6$	40		2.55	31.5	101			
			1.96	29.5	012			
$Na_2Sn(OH)_6$	50	Sb–Sn	3.067	100	200	0.20	–	rhombohedral
$+KSb(OH)_6$	20		2.175	53.8	220			
$+H_2C_4H_4O_6$	40		1.770	31.5	222			
			1.533	20.8	400			
			1.367	25.4	420			
			1.252	22.3	442			

temperature. At a given current density the efficiency increases with increasing antimony content in the bath, even though this increases the cathodic polarization.

In solutions free from tartaric acid (pH 11.2), a white layer, probably of antimony oxide Sb_2O_3, is formed on the anode surface. Very fine-grained and highly adherent greyish deposits are produced on the cathode. X-ray diffraction analysis shows that these deposits are amorphous (Table 1). Similar results have been reported previously on antimony deposits [24]. This behaviour may be explained on the basis that the deposits in this case contain a very small grain size which cannot yield an X-ray diffraction pattern at all. The SEM micrograph given in Fig. 5 confirms this explanation, since the graph shows that the deposit consists of very fine spherical grains in the form of islands, sparsely covering the cathode. The size of these grains is very small, i.e. less than 0.1 μm.

On the other hand, addition of tartaric acid to the solution (pH 7.4) prevents the formation of the anodic layer and at the same time enhances both the darkness and microhardness (Table 2) of the antimony deposits. The addition of the acid may encourage the production of hydrogen and increase the hardness. Moreover, the

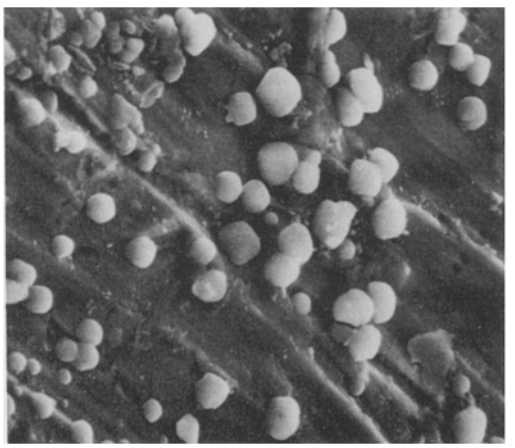

Fig. 5. SEM photographs of antimony electrodeposited on steel for 60 min for 20 g l^{-1} $KSb(OH)_6$ at 0.8 A dm^{-2} and 25° C. × 2100.

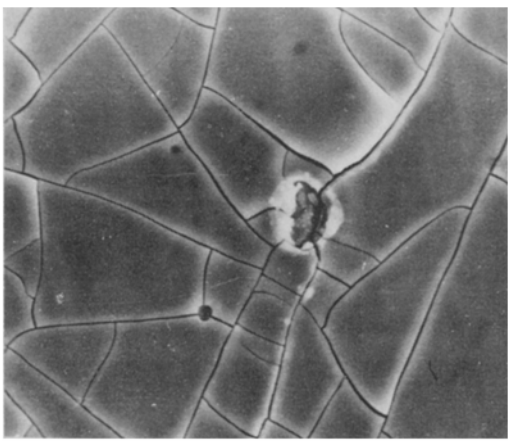

Fig. 6. SEM photographs of antimony electrodeposited on steel for 60 min for 20 g l^{-1} $KSb(OH)_6$ and 40 g l^{-1} $H_2C_4H_4O_6$ at 0.8 A dm^{-2} and 25° C. × 700.

Table 2. Microhardness of Sb and Sb–Sn deposits plated at 0.8 A dm^{-2} and 30° C for 60 min on steel cathodes

Bath	*pH*	*Conc.* ($g\,l^{-1}$)	*Deposit*	*Microhardness (VHN)* ($kg\,m^{-2}$) × 10^{-6}
$KSb(OH)_6$	11.2	20	Sb	220
$KSb(OH)_6$	7.4	20	Sb	272
$+H_2C_4H_4O_6$		40		
$KSb(OH)_6$	7.4	20	Sb–Sn	293
$+Na_2Sn(OH)_6$		50		
$+H_2C_4H_4O_6$		40		

antimony deposits obtained under this condition have the hexagonal crystal structure (Table 1). This modification of the structure may be due to the decrease in the cathodic polarization produced by the addition of the acid to the bath (Fig. 1). The decrease in polarization may retard the nucleation rate and favour the formation of less fine-grained deposits. The SEM photographs of the deposits plated from these solutions are characterized by the presence of cracks as shown in Fig. 6.

Antimony–tin alloys were electroplated from mixtures of $KSb(OH)_6$, $Na_2Sn(OH)_6$ and tartaric acid. In all these baths the pH was kept constant at 7.4. The cathodic potential–current density curves for antimony–tin deposition are given in Figs 7 and 8. According to the data of Fig. 7 it is clear that the cathodic polarization increases with increasing the antimony content of the bath. These results are in agreement with those obtained by Shevts *et al.* [24] during the deposition of this alloy from fluoride bath, where the authors observed that the cathodic overpotential is shifted strongly to a more negative value with an increase in the antimony content in the bath. Data of Fig. 8 reveal that the cathodic polarization of alloy deposition decreases with increasing temperature.

Comparing the polarization curves of the alloy and those of the individual parent metals under similar conditions, it is seen that both the static potential and cathodic polarization of antimony are more positive than those of tin, indicating that antimony behaves as a nobler metal. The alloy curve lies between the curves of the parent metals. This position infers that the

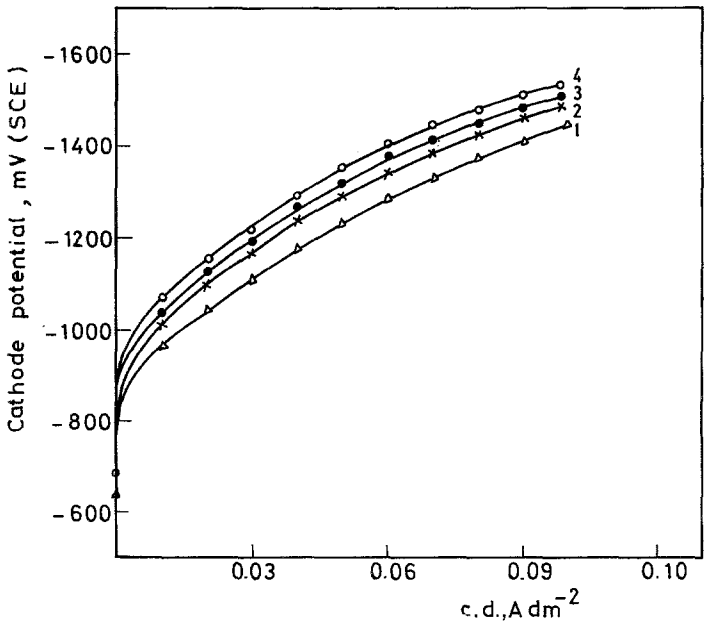

Fig. 7. Cathode polarization of antimony–tin alloy from solutions containing 50 $g\,l^{-1}$ $Na_2Sn(OH)_6$ and 40 $g\,l^{-1}$ $H_2C_4H_4O_6$ at pH 7.4 and 30° C at various concentrations of $KSb(OH)_6$: curve 1, 5 $g\,l^{-1}$; curve 2, 15 $g\,l^{-1}$; curve 3, 20 $g\,l^{-1}$; curve 4, 25 $g\,l^{-1}$.

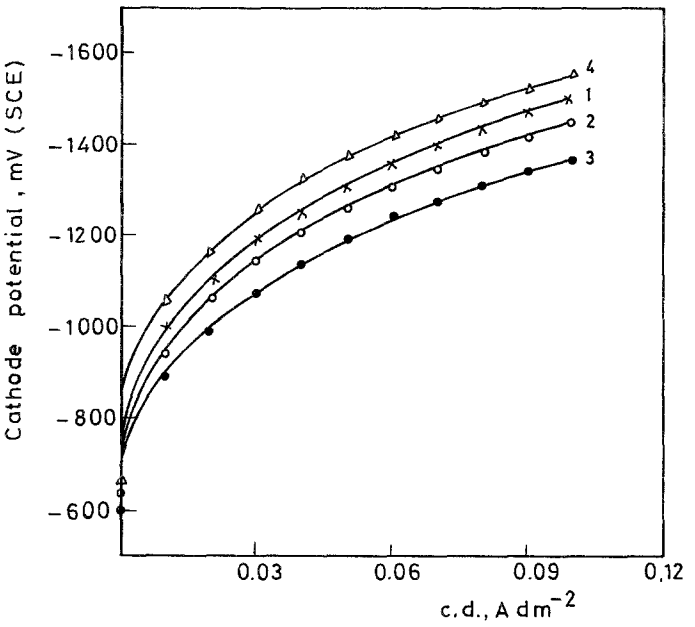

Fig. 8. Cathodic polarization curves. Curve 1, antimony–tin from solution containing 20 g l^{-1} $KSb(OH)_6$ + 50 g l^{-1} $Na_2S(OH)_6$ + 40 g l^{-1} $H_2C_4H_4O_6$, at pH 7.4, 30° C. Curve 2, antimony–tin from solution containing 20 g l^{-1} $KSb(OH)_6$ + 50 g l^{-1} $Na_2Sn(OH)_6$ + 40 g l^{-1} $H_2C_4H_4O_6$, at pH 7.4, 50° C. Curve 3, antimony from solution containing 20 g l^{-1} $KSb(OH)_6$ + 40 g l^{-1} $H_2C_4H_4O_6$, at pH 7.4, 30° C. Curve 4, tin from solution containing 50 g l^{-1} $Na_2Sn(OH)_6$ + 40 g l^{-1} $H_2C_4H_4O_6$, at pH 7.4, 30° C.

codeposition enabled tin (the less noble metal) to deposit at more positive potentials and caused antimony (the more noble metal) to deposit at more negative potentials than in the individual deposition cases.

Fig. 9 illustrates the effect of increasing the antimony content of the bath on the total efficiency of the alloy deposition and on the partial efficiencies of both antimony and tin (the broken lines) in each alloy. Inspection of these curves reveals that the total efficiency of the alloy deposition is less than 100% as a result of hydrogen evolution. The efficiency of the codeposition decreases at first and then tends to increase with increasing antimony content of the bath. This behaviour is the result of the decrease

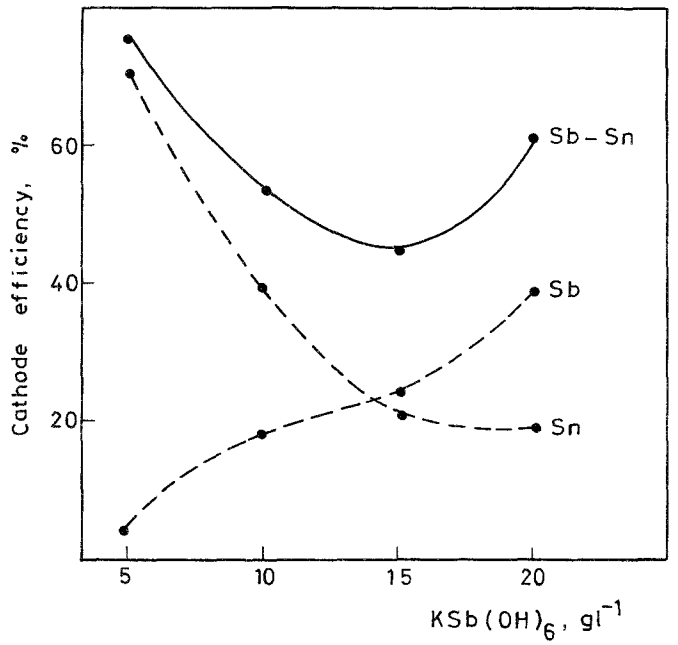

Fig. 9. Cathode efficiency of antimony–tin alloys and partial current efficiencies of antimony and tin in the alloys (broken lines) at 0.8 A cm^{-2}, 30° C and plating time 60 min from a solution containing 50 g l^{-1} $Na_2Sn(OH)_6$ + 40 g l^{-1} $H_2C_4H_4O_6$ + varying concentrations of $KSb(OH)_6$ at pH 7.4.

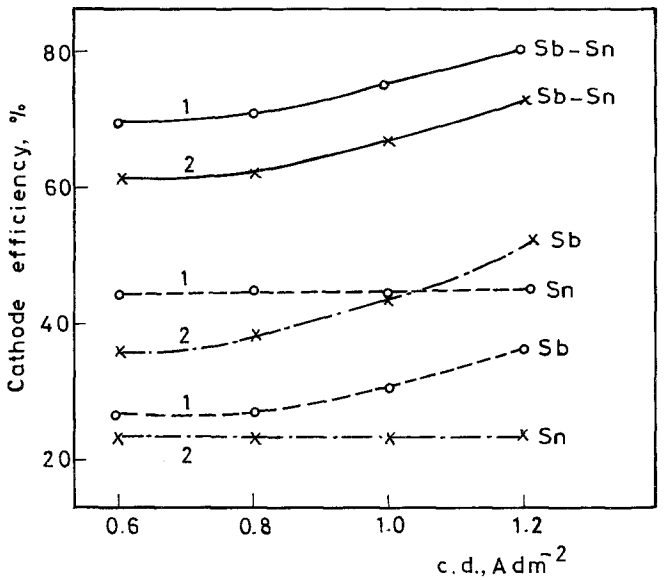

Fig. 10. Cathodic current efficiency of antimony–tin alloys and partial current efficiencies of antimony and tin in the alloys (broken lines) from a solution containing $20\,g\,l^{-1}$ $KSb(OH)_6$ + $50\,g\,l^{-1}$ $Na_2Sn(OH)_6$ + $40\,g\,l^{-1}$ $H_2C_4H_4O_6$ at pH 7.4. Plating time was 60 min; curve 1 30° C; curve 2, 50° C.

in the partial efficiency of tin deposition and the increase in the partial efficiency of antimony deposition. This trend in the variation of the partial current efficiencies is in such a direction as to increase the antimony content of the deposit.

Fig. 10 presents the cathodic current efficiency for the alloy deposition at 30 and 50° C as a function of current density. Comparison of the partial efficiencies of the parent metals in the alloy shows that the principal influence of the current density is to increase the efficiency of antimony deposition without appreciably affecting the efficiency of tin deposition. Careful examination of the data in Fig. 10 shows that the codeposition efficiency increases with increasing bath temperature. This behaviour is the result of the larger increase in the partial efficiency of tin deposition and the smaller decrease in the partial efficiency of antimony deposition.

Fig. 11 shows the percentage of antimony in the deposit against its metal content of the bath at 30° C. As expected from Fig. 9 the percentage of antimony in the deposit increases with increase of its content in the bath. This is consistent with Brenner's [22] observation that an

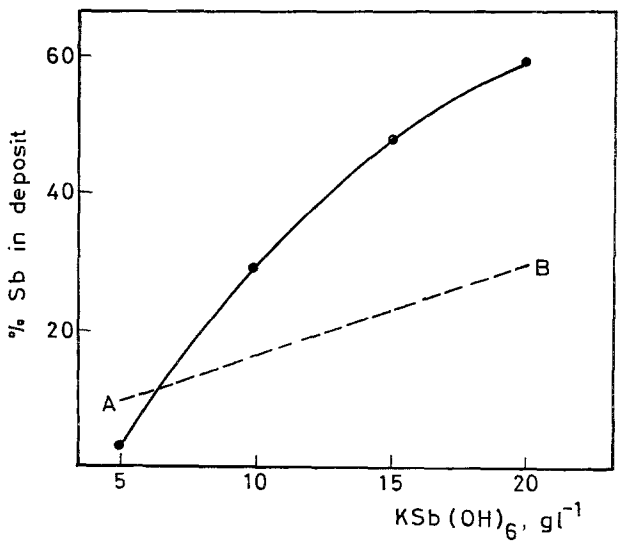

Fig. 11. The percentage of antimony in the deposits plated from solution containing $50\,g\,l^{-1}$ $Na_2Sn(OH)_6$ + $40\,g\,l^{-1}$ $H_2C_4H_4O_6$ + varying concentrations of $KSb(OH)_6$ at pH 7.4, 30° C and $0.8\,A\,dm^{-2}$. Plating time was 60 min. The broken line, AB, represents the percentage of antimony in the solution.

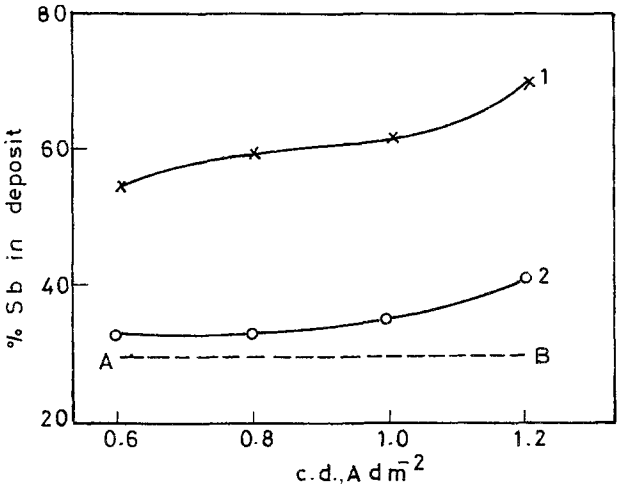

Fig. 12. The percentage of antimony in the deposit plated from solution containing 50 g l^{-1} $Na_2Sn(OH)_6$ + 20 g l^{-1} $KSb(OH)_6$ + 40 g l^{-1} $H_2C_4H_4O_6$ at pH 7.4. Plating time was 60 min; curve 1, 30° C; curve 2, 50° C. The broken line, AB, represents the percentage of antimony in the solution.

increase in the metal percentage of a parent metal in the plating bath results in an increase in the percentage of that metal in the deposit. The main characteristic of the curves of Fig. 11 is that the percentage of antimony in the alloy lies above its reference composition AB; the latter represents the percentage of antimony in the bath. This result implies that antimony (the more noble) is preferentially deposited.

The curves of Fig. 12 depict the influence of increasing both the current density and temperature on the percentage of antimony in the alloy deposits. It is clear that this percentage increases with increasing current density. The magnitude of the increase in the alloy composition is small. Such variation of the alloy composition with the current density denotes that the codeposition is of an irregular type [22]. However, the percentage of antimony in the deposit decreases with temperature This trend is also consistent with the behaviour of the irregular alloy plating system.

Fine-grained, highly adherent and dark-greyish deposits with metallic lustre were obtained from the above-mentioned solutions. The darkness increases with increasing the antimony content of the deposit. The microhardness of the as-plated alloys is greater than that of the individual deposited antimony as shown in Table 2. X-ray diffraction patterns given in Table 1 reveal that antimony–tin (58% antimony) alloy has a rhombohedral crystal structure. An SEM micrograph of the as-plated antimony–tin (58% antimony) alloy is given in Fig. 13. A very dense, dark layer is observed which consists of small grains less than 1.0 μm in size and free from cracks. These grains are randomly distributed and pile on each other to cover the substrate to a high degree.

4. Conclusions

Fine-grained, dark-greyish and highly adherent antimony plates can be deposited onto steel substrates from $KSb(OH)_6$ solutions. The cathode current efficiency is low as a result of hydrogen evolution. The efficiency increases with

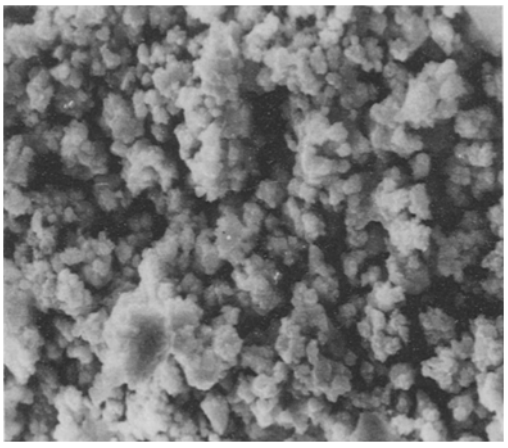

Fig. 13. SEM photographs of antimony–tin electrodeposited on steel for 60 min from 50 g l^{-1} $Na_2Sn(OH)_6$, 20 g l^{-1} $KSb(OH)_6$ and 40 g l^{-1} $H_2C_4H_4O_6$ at 0.8 A dm^{-2} and 25° C. × 2100.

increasing current density and decreases with temperature. Addition of tartaric acid to the bath increases the darkness and microhardness of the deposits.

Antimony–tin alloy plates can be deposited from mixtures of $KSb(OH)_6$, $Na_2Sn(OH)_6$ and tartaric acid. In these solutions antimony is nobler than tin and is preferentially deposited. The codeposition process belongs to an irregular alloy plating system. The antimony content of the deposits increases with increasing both current density and antimony content of the bath but decreases with temperature. X-ray diffraction analysis shows that the alloy can be deposited with the rhombohedral crystal structure.

References

[1] Y. N. Sadana, J. P. Singh and K. Kumar, *Surf. Technol.* **24** (1985) 319.
[2] G. D. Parkes, 'Modern Inorganic Chemistry', Longmans, Harlow (1967) p. 845.
[3] N. P. Fedot'ev, S. Ya. Grilikhes and I. B. Naryshkina, *Zh. Prikl. Khim.* **32** (1959) 2798.
[4] K. G. Soderberg and H. L. Pinkerton, *Plating* **37** (1950) 254.
[5] V. N. Medyanik and G. V. Shula, *Zh. Prikl. Khim.* **49** (1976) 1081.
[6] Z. A. Solov'eva, L. N. Solodkova and A. T. Vagramyan, *Elektrokhimiya* **6** (1970) 590.
[7] L. N. Solodkova, Z. A. Solov'eva and G. M. Plavnik, *ibid.* **10** (1974) 849.
[8] A. H. Dukose, *Proc. Amer. Electroplater's Soc.* (1956) 151.
[9] V. N. Lebedeva and M. Ya. Popereka, *Electrokhimiya* **1** (1965) 743.
[10] G. S. Rao, R. K. Lyer and S. G. Deshpande, *Indian J. Technol.* **10** (1972) 275.
[11] C. Marzano and R. S. Modjeska, *Tech. Proc. Amer. Electroplater's Soc.* **49** (1962) 95.
[12] J. W. Cuthbertson and N. Parkinson, *J. Electroplater's Tech. Soc.* **28** (1952) 195.
[13] N. T. Kudryavtsev, K. M. Tyutina and M. M. Yarlykov, *Tr. Mosk. Khim. Technol. Inst.* **26** (1959) 120.
[14] V. V. Bogoslovskii, K. M. Tyutina and N. T. Kudryavtsev, *ibib.* **75** (1973) 200.
[15] V. G. Kushnir, E. P. Zhelibo, V. V. Myalkovskii and T. M. Shevtz, *Ukr. Khim. Zh.* **44** (1978) 372.
[16] O. V. Izbekova, I. V. Dema and N. I. Vrzhosek, *Vism. Kiiv. Politekh. Inst. Ser. Khim. Mashinobuduu. Takhnol.* **14** (1977) 108.
[17] R. G. Monk and H. G. T. Ellingham, *J. Electrodepositer's Tech. Soc.* **11** (1936) 39.
[18] S. S. Abd El Rehim and M. E. El Ayashy, *J. Appl. Electrochem.* **8** (1978) 33.
[19] S. S. Abd El-Rehim, *ibid.* **8** (1978) 569.
[20] S. S. Abd El Rehim, S. M. Abd El Wahaab and O. M. Abd Ella, *Surf. Technol.* **21** (1984) 245.
[21] S. S. Abd El Rehim, A. M. El Halim and M. M. Osman, *ibid.* **22** (1984) 337.
[22] *Idem, J. Appl. Electrochem.* **15** (1985) 107.
[23] A. Brenner, 'Electrodeposition of Alloys', Vol. 1, Academic Press, New York (1963).
[24] T. M. Shevts, E. P. Zhelibo and V. G. Kushniv, *Electrokhimiya* **14** (1978) 1106.